

**GROUND-BASED TECHNOLOGIES FOR COTTON ROOT ROT CONTROL: AN UPDATE**

**Curtis D. Cribben**  
**J. Alex Thomasson**  
**Yufeng Ge**  
**Matthew D. Korte**  
**Cristine L.S. Morgan**  
**Texas A&M University**  
**College Station, TX**  
**Chenghai Yang**  
**USDA ARS**  
**Weslaco, TX**  
**Robert L. Nichols**  
**Cotton Incorporated**  
**Cary, NC**

**Abstract**

The overall goal of this research is to develop ground-based technologies for early detection and site-specific management of CRR (cotton root rot). Early detection could facilitate a more economical solution than those that might be used after plant infection had become more severe and widespread. Three cotton fields around CRR-prone areas of Texas have been the sites for two years of data collection. Freshly picked cotton leaves from healthy, disease-stressed, and dying or dead plants were scanned with an ASD VisNIR spectroradiometer. Surface soil moisture, temperature, and electrical conductivity were measured in each field with a Delta-T WET sensor. A thermal infrared camera was used to capture leaf canopy images of healthy and disease-stressed plants. A complete soil ECa (apparent electrical conductivity) survey was conducted for each field with an EM-38 sensor. Plant status was visually inspected and recorded to form a series of disease-progression maps in each field. Preliminary models relating ECa and remotely sensed NDVI (normalized difference vegetative index) levels to CRR incidence produced varying results, which may be improved through further analysis. Leaf spectra have also been evaluated with LDA (linear discriminant analysis) to classify their infection level with a 66% success rate. These data continue to be analyzed to (1) identify promising means for early detection of CRR, (2) relate disease occurrence to soil data, and (3) develop sound strategies for site-specific management of CRR.

**Introduction**

*Phymatotrichopsis omnivora*, otherwise known as cotton root rot (CRR), is a highly destructive fungus affecting dicotyledonous plants in the southwestern United States and northern Mexico (Uppalapati et al., 2010). CRR penetrates the roots of broadleaf plants and blocks the flow of water from the roots to the leaves for transpiration, causing the leaves to wilt (Yang et al., 2005). In general the fungus will not infect entire fields (Lyda, 1978); instead it will begin from different locations throughout the field and spread in a circular pattern from those foci (Uppalapati et al., 2010). Due to the added stress the fungus puts on the plant, infected plants usually produce a lower lint yield and lower quality cotton than healthy plants from the same field (Ezekiel and Taubenhaus, 1934; Taubenhaus and Ezekiel, 1935). Yield and quality are the principal determiners of profitability in cotton production, meaning that CRR can have serious effects on profitability.

Much work has been done concerning the life cycle, treatment methods, and remote-sensing identification of CRR. Sclerotia are the food-storage bodies of the fungus, which allow it to lie dormant in the soil from one growing season to the next (Neal, 1929). The remainder of the life cycle is described by Uppalapati et al. (2010) in the following process. Thin strands called hyphae will branch out from the sclerotia in search of an additional nutrient source or host. As more and more hyphae branch out of the sclerotia they begin to form thicker bundles called mycelium. Upon contact with a host root the mycelial strands unbind and allow the individual hyphae to engulf and penetrate the root. Once the host plant has died, the hyphal strands on the root's surface branch out to find a new host or begin to form new sclerotia in order to complete the life cycle.

The widespread effects of CRR have brought about several treatment methods with limited success. Cotton plant roots with lower carbohydrate concentrations were been shown to be more susceptible to CRR, but no cost-effective method for raising the concentrations was found (Eaton and Rigler, 1946). Lyda(1978) references Shear (1907 and 1908) when discussing how carbon dioxide in the soil facilitates the growth of CRR while simultaneously

suppressing the growth of competing saprophytes. Based on this idea, many have used deep plowing to aerate the soil to minimize the occurrence of CRR, but disease development is slowed only temporarily (Lyda, 1978). Several chemical compounds have also been examined for their influence on disease spread. Sodium chloride was found to be effective in lowering disease incidence in soils known to be infested with the fungus (Taubenhaus et al., 1932). Furthermore, a positive correlation exists between high levels of exchangeable sodium in the soil and the absence of CRR (Lyda and Kissel, 1974). Recently, Isakeit et al. (2010) have explored methods involving the chemical flutriafol, which has been successful in reducing the effects of CRR.

In an effort to increase the economic feasibility of potential treatment methods, Yang et al. (2005) used the following steps to identify problem areas in specific fields with remote sensing. Aerial images of a cotton field's canopy in three color bands (near infrared, red, and green) were classified into areas of healthy or diseased plants, assuming that the main stress present was CRR. The resulting disease maps were modified to remove healthy areas too small for farm equipment to practically avoid. A buffer zone was then added around the infected areas to account for disease spread. The final maps served to display treatment areas of the cotton field for precision application.

Previous research has not as yet produced a foolproof cost-effective solution for the identification and precision treatment of CCR. The objectives of this project are thus first to understand the progression of CRR in a field both temporally and spatially, and second to develop a ground-based method and sensor for early detection of plant infection. This paper will focus on the most recently completed research concerning both objectives.

### **Materials and Methods**

Three plot locations were chosen for the collection of data during the 2010 and 2011 growing seasons. The first plot was located on the Stiles Farm and Texas A&M Research Center at Thrall, in the Northern Blackland Prairie of Texas. The second plot was located near Sinton, TX and falls in the Southern Subhumid Gulf Coastal Prairies of Texas. The third plot was located in the Red Prairies of Texas near San Angelo. The three plots measured 24 rows wide by approximately 45 yards (45 paces) long, and data collection for the each location was based on a weekly schedule. A detailed description of the data collected during each plot visit is discussed in Cribben et al., 2011.

An apparent electrical conductivity (ECa) survey was conducted over a large portion of the field at each of the three locations after the 2010 growing season with an EM-38 sensor (Geonics Limited, Mississauga, Ontario, Canada). The EM-38 was pulled through every sixth row of the three sample areas to obtain a uniform distribution of data. Vertical measurements with the EM-38 were taken straight down into the soil, whereas horizontal measurements recorded the EM-38's response to more shallow soil with a wider span. The results of each survey were mapped with ArcGIS (ESRI, Redlands, CA), and the ECa values were divided into three equal categories representing the high, middle, and low thirds of conductivity in each field. The ECa maps were superimposed over aerial images of each field obtained with the method described in Yang (2010). Soil coring points were placed at locations of different conductivity and/or disease incidence in order to identify which soil properties were associated with these differences.

Approximately 24 soil coring points were chosen at each of the three sites and collected with a soil coring truck equipped with a Giddings Probe (Giddings Machine Company, Windsor, CO). Collected cores were analyzed with respect to soil horizons and presence of calcium carbonates. Particle size analysis and other tests will be conducted later.

Leaf samples were taken at every fifth pace of every third row during each plot visit throughout both growing seasons. Reference leaves were also collected to provide examples of the disease progression from healthy to dead on a one-to-four scale. Leaves were collected at the plot and stored in plastic zipper bags which were placed inside a cooler on ice. Once all samples were collected, the cooler was taken back to the lab where the leaves were analyzed. The leaf collection procedure was based on a study done by Thomasson and Sui (2009) that proved this method to have minimal effects on leaf reflectance spectra within six hours of picking. Each leaf was then scanned twice with the ASD VisNIR spectroradiometer to give the reflectance signature that would be used to classify the leaves. The reference leaf spectra were then put through a linear discriminant analysis to identify which bands of the spectrum could best classify leaf spectra into the correct category on the one-to-four scale.

At the end of the 2011 growing season cotton samples were hand harvested at the San Angelo location to provide information on the economic impact of CRR. Prior to defoliant application 24 points within the field were identified as either infected or healthy. Approximately two weeks after defoliant application one thousandth of an acre was hand harvested at each of the 24 points. 160 gram subsamples from each point were ginned at the Cotton Improvement Laboratory at Texas A&M University to obtain yield data. Three 10 gram replicates were taken from each subsample and sent to Cotton Incorporated for HVI testing. The HVI data were analyzed to determine whether a significant difference between healthy and infected plants existed.

### Results and Discussion

Eca surveys and aerial images were the starting point for understanding the behavior of CRR on a large scale. ArcGIS maps of the Sinton location provide an example of how the EM-38 information was utilized. From the aerial image on the right of figure 1, the circular pattern of CRR is clearly seen in violet, whereas the healthy plants are shown in green. The Eca map on the left has been divided into high, medium, and low thirds of conductivity represented by red, orange, and yellow colors, respectively. Correlation analysis was conducted between average Eca and average NDVI for each 15-m by 15-m cell in the image at right. The San Angelo site gave an  $r^2$  of 0.372 for this analysis, but neither Thrall nor Sinton approached that value. This low  $r^2$  implies that soil Eca can not directly map CRR incidence, but that maybe in some instances there is a weak relationship.

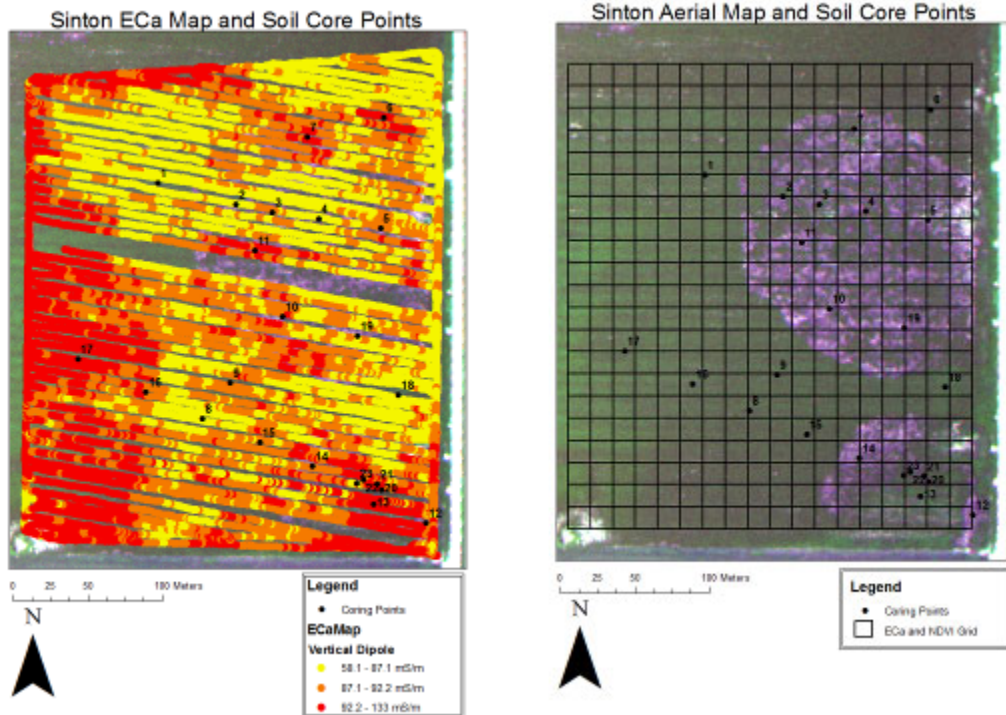


Figure 1 Eca map (left) and aerial image (right) of the Sinton field.

The black numbered points in figure 1 are the soil coring points throughout the surveyed area. Cores were taken down to the soil's parent material at each point and taken back to the lab for analysis. Once the cores were classified by horizon in the laboratory, the soil horizon depths were analyzed with respect to Eca within a nine meter radius of the coring point. Similarly, the depths of calcium carbonate traits were recorded and analyzed with respect to Eca at each core. None of the correlations was significant. More analyses will be conducted to determine whether soil properties discernible in soil-cores are being mapped by the EM-38. If certain soil properties are identified, their influence on CRR will be examined to determine whether soil Eca can be better related to the spread of disease.

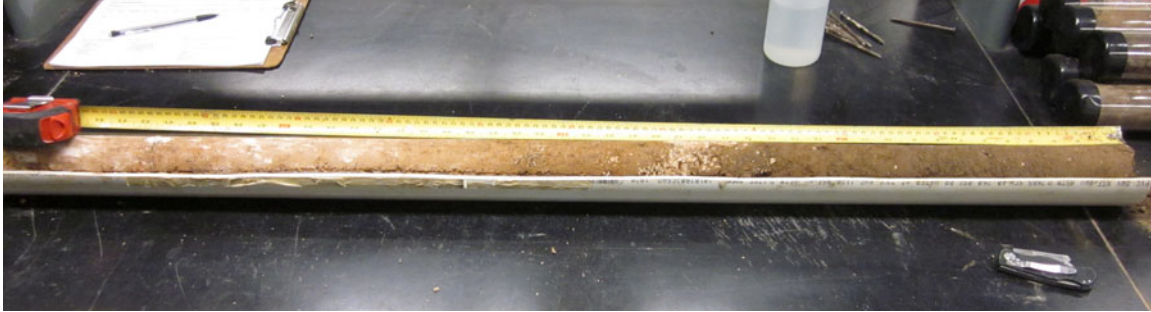


Figure 2 An example of a soil core taken from the San Angelo location.

Linear discriminant analysis was used to establish wavelength ranges that can eventually be used in sensor design. The models produced from these data were evaluated for accuracy by determining the percentage with which each model could predict a leaf's category on the one-to-four scale. Also, the categories of 2 through 4 were combined into a single category representing leaves with some degree of infection, and those were compared to the category 1 leaves that were considered completely healthy. The results of the best model of each of these types can be seen in tables 1 and 2.

Table 1 Known leaf categories (axis on left) compared with computer-predicted categories (axis along top).

		predicted			
		1	2	3	4
actual	1	41	9	0	0
	2	12	27	5	1
	3	4	9	29	7
	4	0	4	12	42

The model used to create table 1 consisted of 50nm wide bands centered at 525nm, 825nm, 1175nm, and 1925nm. The accuracy of this model can be found by adding the number of samples where the actual category of the leaf matches the computer predicted category and dividing by the total number of samples. Completing this calculation gives an accuracy of 68.8%.

Table 2 Category 1 leaves (healthy, H) compared with all categories of infected leaves (I, categories 2 through 4).

		predicted	
		H	I
actual	H	35	15
	I	5	147

The model used to create table 2 consisted of 50nm bands centered at 525nm, 2075nm, 2175nm, and 2325nm. This model correctly classified the health of a leaf 90.0% of the time. The next step in sensor design is to determine the best center wavelengths and band widths to create an accurate and cost-effective optical sensor.

The application of an optical sensor in practical cotton growing processes that might include CRR treatment requires some explanation. The current chemical treatment method being pursued for producer use involves a fungicide

treatment to each furrow at planting. This method limits the timing of CRR treatment to once each season as the field is planted. It does not appear that alternative treatment methods or timings will be permitted in the near future due to the lack of research concerning midseason treatments. As a result, the most promising application for an optical sensor exists during the defoliation process. By mounting sensors to the sprayer boom during defoliant application the full extent of CRR could be mapped without additional passes through the field. A map generated with such data could serve as a guide during the subsequent planting season to limit fungicide application to at-risk areas.

During the 2011 growing season cotton samples were collected from the San Angelo location to obtain fiber quality data related to CRR. The six fiber-quality properties in which a significant difference existed between healthy and infected cotton plants were micronaire, uniformity, length, strength, yellowness, and short fiber content. Each of these showed the healthy cotton plants as producing higher quality cotton. The two categories that did not have a significant difference between the data sets were elongation and reflectance. These results are in agreement with previously reported data.

### Conclusions

Three important conclusions can be drawn from the recently completed research:

- ECA maps and CRR incidence are not highly correlated, but further study of soil properties through analysis of soil cores may aid in understanding the relationship.
- A four-band spectral model of leaf reflectance has the capability to distinguish between healthy and infected cotton leaves with 90.0% accuracy.

### Acknowledgements

The authors of this paper would like to thank Cotton Incorporated and the Texas state Support Committee for providing funding for this project. Also, a special thanks goes out to Mr. Miles Moudy, all of Dr. Cristine Morgan's students, and the producers and extension agents for helping with data collection.

### References

- Cribben, C.D., J.A. Thomasson, Y. Ge, M.D. Korte, C.L.S. Morgan, C. Yang, R.L. Nichols. 2011. Ground-based technologies for cotton root rot control. *Beltwide Cotton Conf. Proc.*, 552-558. Cordova, TN: National Cotton Council.
- Eaton, F.M., N.E. Rigler. 1946. Influence of carbohydrate levels and root-surface microfloras on phymatotrichum root rot in cotton and maize plants. *Journal of Agricultural Research* 72(4): 137-161.
- Ezekiel, W.N., J.J. Taubehaus. 1934. Cotton crop losses from phymatotrichum root rot. *J. Agric. Res.* 49(9): 843-858.
- Isakeit, T., R. Minzenmayer, A. Abrameit, G. Moore, J.D. Scasta. 2010. Control of phymatotrichopsis root rot of cotton with flutriafol. *Beltwide Cotton Conf. Proc.*, 200-203. Cordova, TN: National Cotton Council.
- Lyda, S.D.. 1978. Ecology of phymatotrichum omnivorum. *Ann. Rev. of Phytopathol.* 16: 193-209.
- Lyda, S.D., D.E. Kissel. 1974. Sodium influence on disease development and sclerotial formation by phymatotrichum omnivorum. *Proc. of the Am. Phytopathol. Soc.*, 163-164. St. Paul, MN: APS Press.
- Neal, D.C. 1929. The occurrence of viable cotton root-rot sclerotia in nature. *Science* 70(1817): 409-410.
- Taubehaus, J.J. W.N. Ezekiel. 1935. The quality of lint and seed from cotton plants with phymatotrichum Root Rot. *Phytopathology* 25: 104-113.
- Taubehaus, J.J. W.N. Ezekiel, J.F. Fudge. 1932. Incidence of root rot as affected by field additions of fertilizer and other salts to the soil. *Texas Agric. Exp. Station Ann. Reports.* 45: 70.

Thomasson, J.A., R. Sui. 2009. Cotton leaf reflectance changes after removal from the plant. *J. Cotton Sci.* 13: 206-211.

Uppalapati, S.R., C.A. Young, S.M. Marek, K.S. Mysore. 2010. Phymatotrichum (cotton) root rot caused by phymatotrichopsis omnivora: retrospects and prospects. *Molecular Plant Pathology* (2010) 11(3): 325-334.

Yang, C. 2010. An airborne four-camera imaging system for agricultural applications. ASABE Paper No. 10-08855. St. Joseph, Mich.: ASABE.

Yang, C., C.J. Fernandez, J.H. Everitt. 2005. Mapping phymatotrichum root rot of cotton using airborne three-band digital imagery. *Trans. ASABE* 48(4): 1619-1626.